Fluorescence Resonance Energy Transfer (FRET) in Microemulsions Composed of Tripled-Chain Surface Active Ionic Liquids (SAILs), RTILs and Biological Solvent: An Excitation Waveleng...

ARTICLE *in* THE JOURNAL OF PHYSICAL CHEMISTRY B · JULY 2013

Impact Factor: 3.3 · DOI: 10.1021/jp405919y · Source: PubMed

THE JOURNAL OF PHYSICAL CHEMISTRY B

Article

pubs.acs.org/JPCB

Fluorescence Resonance Energy Transfer in Microemulsions Composed of Tripled-Chain Surface Active Ionic Liquids, RTILs, and Biological Solvent: An Excitation Wavelength Dependence Study

Chiranjib Banerjee, Niloy Kundu, Surajit Ghosh, Sarthak Mandal, Jagannath Kuchlyan, and Nilmoni Sarkar*

Department of Chemistry, Indian Institute of Technology, Kharagpur 721302, WB, India

ABSTRACT: In this article we have reported the fluorescence resonance energy transfer (FRET) study in our earlier characterized surface active ionic liquids (SAILs)-containing microemulsion, i.e., *N*-methyl-*N*-propylpyrrolidinium bis(trifluoromethanesulfonyl)imide ($[P_{13}][Tf_2N]$)/[CTA][AOT]/isopropyl myristate ([IPM]) and *N*,*N*,*N*-trimethyl-*N*-propylammonium bis(trifluoromethanesulfonyl)imide ($[N_{3111}][Tf_2N]$)/[CTA][AOT]/[IPM] microemulsions (Banerjee, C.; Mandal, S.; Ghosh, S.; Kuchlyan, J.; Kundu, N.; Sarkar, N. *J. Phys. Chem. B* **2013**, *117*, 3927−3934). The occurrence of effective FRET from the donor, coumarin-153 (C-153) to the acceptor rhodamine 6G (R6G) is evident from the decrease in the steady state fluorescence intensity of the donor with addition of acceptor and subsequent increase in the fluorescence intensity of the acceptor in the presence of donor. The excitation wavelength dependent FRET from C-153 to R6G has also been performed to assess the dynamic heterogeneity of these confined systems. In time-resolved experiments, the significant rise time of the acceptor in the presence of the donor further confirms the occurrence of FRET. The multiple donor−acceptor (D−A) distances, for various microemulsions, obtained from the rise times of the acceptor emission in the presence of a donor can be rationalized from the varying distribution of the donor, C-153, in the different regions of the microemulsion. Time-resolved measurement reveals that with increasing excitation wavelength from 408 to 440 nm, the contribution of the faster rise component of FRET increases significantly due to the close proximity of the C-153 and R6G in the polar region of the microemulsion where occurrence of FRET is very high. Moreover, we have also studied the FRET with variation of *R* (*R* = [room temperature ionic liquids (RTILs)]/[surfactant]) and shown that the effect of excitation wavelength on FRET is similar irrespective of *R* values.

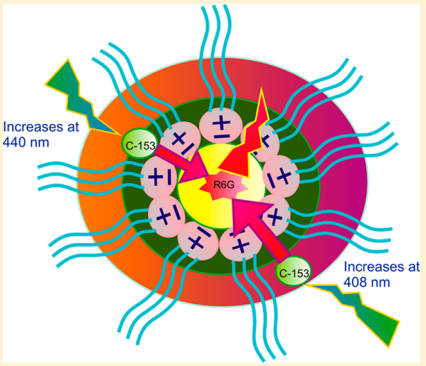

1. INTRODUCTION

Room temperature ionic liquids (RTILs) have attracted a lot of recent attention due to their unusual properties.[1−3] They are environmentally benign, nontoxic green solvents, with melting points below room temperature.[4] Their unique properties and the rising necessity of sustainable "green" chemistry have also led to an unparalleled increase in interest in such salts. Most investigations on RTILs are partly due to their potential environmentally benign nature. RTILs are organic salts composed entirely of ions, and unlike the common organic salts, which melt at high temperatures, these salts melt at considerable low temperature primarily due to the presence of sterically mismatched ions.[5,6] Since the properties of RTILs are very much dependent on their constituent ions, it is possible to obtain a RTIL of a desired property by tuning the cationic and anionic constituents; such liquids are called "designer solvents".[7,8] In our previous work, we have synthesized surface active ionic liquid (SAIL), $[C_4mim][AOT]$, by an anion exchange reaction between NaAOT and 1-butyl-3-methylimidazolium bromide ($[C_4mim][Br]$) and we showed that a huge number of IL-in-oil microemulsions can be prepared just by replacing the inorganic cation, Na^+ of NaAOT, by any organic cation and using different ionic liquids as the polar core.[9] As an effort toward this, we have recently prepared two more SAILs, [CTA][AOT] and [BHD][AOT], by replacement of Na^+ with long-chain cations.[10] In [CTA][AOT] the cation of AOT has been replaced by cetyltrimethylammonium ion and in [BHD][AOT] the same cation is replaced by benzyl-*n*-hexadecyldimethylammonium ion, yielding a highly viscous liquid in the former and a comparatively low viscous liquid in the latter. These SAILs show very different properties from the original surfactants and studies on the properties of the self-assembled aggregates in aqueous as well as nonaqueous solutions formed with this kind of SAILs are scarce.

Fluorescence resonance energy transfer (FRET) was used as a probe for single mismatches in DNA hybridization[11] and dynamics of DNA replication and telomerization,[12] as well as to study inhibition assays based on the modulation of FRET efficiencies.[13] FRET pairs provide information about donor−acceptor distance distributions, receptor−ligand binding, and macromolecule conformation.[14,15] This distance-dependent behavior has provided a highly effective tool for studying the

Received: June 15, 2013
Revised: July 15, 2013
Published: July 18, 2013

dx.doi.org/10.1021/jp405919y | *J. Phys. Chem. B* 2013, 117, 9508−9517

Scheme 1

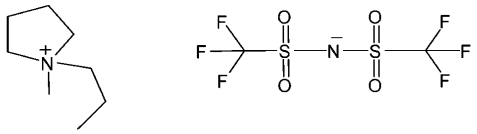

N-methyl-N-propylpyrrolidinium bis(trifluoromethanesulfonyl)imide, ([P_{13}][TF_2N])

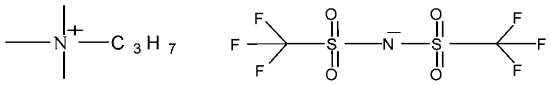

N,N,N-trimethyl-N-propylammonium bis(trifluoromethanesulfonyl)imide, ([N_{3111}][TF_2N])

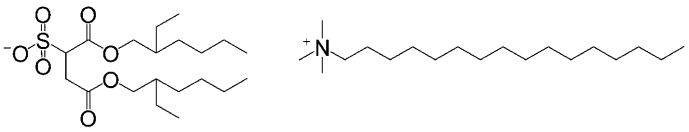

[CTA][AOT]

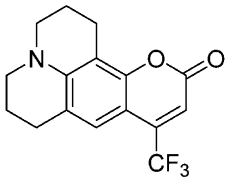

Coumarin 153

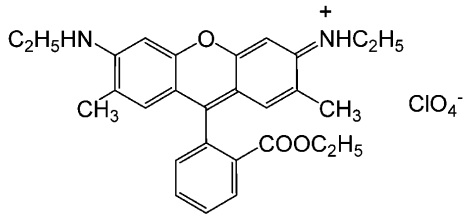

Rhodamine 6G (R6G)

structure and dynamics of large molecules in the condensed phases for physicists, chemists, and biologists. The Förster theory in energy transfer (ET) predicts a negative sixth root dependence of the ET efficiency on the D−A separation distance and requires a linear proportionality of the ET efficiency on the overlap integral.[16,17] However, a recent report shows evidence for a negative-sixth to negative-fourth power dependence on distance, depending on the nature of the constituents.[18] According to the calculations of Scholes et al.[19] in photosynthetic systems and Wong et al.[20] in conjugated polymers, it is clear that the rate of FRET shows a much weaker distance dependence ($\sim R_{DA}^{-2}$) when the distance between donor and acceptor is very small (~10 Å). Fleming and co-workers[21−23] have suggested that in aggregated systems where multiple donors and acceptors are confined at a very short distance of separation the Förster theory in its standard form is found to be invalid. It was also demonstrated that in short-range ET, from quantum dots (QDs) to molecular energy acceptors, other parameters appear to play a role in addition to the Förster mechanism.[24,25] Such non-Förster-type parameters for QD conjugates involve among others the effects of surface variations, degree of interdigitization, and contributions of surface states. In recent years, the ultrafast FRET at short distances has gained a lot of attention.[26−29] Bhattacharyya et al. have shown that if the donor and acceptor are isolated by surfactant chains, then Förster theory remains valid at very short distances.[30] They have monitored ultrafast FRET in cationic vesicles,[30] micelles,[31,32] mixed micelles,[33] and micro-emulsions,[34] and stated that the Förster theory provides a good estimate of the measured donor−acceptor distance due to the intervening surfactant chains.

Microemulsions are optically transparent, isotropic, thermodynamically stable solution mixtures of at least three components, namely, two immiscible solvents and a surfactant. Kahlweit et al. studied numerous systematic experiments to generalize the behavior of microemulsions.[35−38] In the recent past, attempts have been made to prepare and study waterless reverse micelles where water has been replaced by polar solvents, which have relatively high dielectric constants and are immiscible in hydrocarbon solvents. These nonaqueous microemulsion systems are superior to the aqueous ones particularly because they can be used as good reaction media. Han and co-workers first discovered that 1-butyl-3-methyl-imidazolium tetrafluoroborate ($bmimBF_4$) assembled in polar nanosized droplets when dispersed in cyclohexane as solvent, and the RTIL microemulsions showed a regular swelling behavior similar to water-in-oil (W/O) microemulsions; that is, the volume of the dispersed nanodroplets is directly proportional to the amount of added RTIL.[39] Several groups prepared and characterized RTILs containing micelles and micro-emulsions.[40−48] Recent attempts have been made to construct microemulsions comprising the pharmaceutically acceptable components Tween-80/butyl lactate/isopropyl myristate (IPM)/water.[49−52] In the present scheme of work, we used IPM instead of cyclohexane or benzene as a nonpolar solvent due to its biocompatibility along with higher boiling point. Very

dx.doi.org/10.1021/jp405919y | J. Phys. Chem. B 2013, 117, 9508−9517

recently, we demonstrated a strategy by which we can formulate IL-in-oil microemulsions exhibiting stability over a wide range of temperatures (278 to ≥423 K) using IPM as a nonpolar solvent.[53]

In this paper, we have investigated FRET in different regions of our previously characterized RTIL-containing microemulsions ([P_{13}][Tf_2N]/[CTA][AOT]/[IPM], [N_{3111}][Tf_2N]/[CTA][AOT]/[IPM]).[10] We have chosen Coumarin (C-153, Scheme 1) as a donor and an ionic dye and Rhodamine 6G (R6G, Scheme 1) as the acceptor molecules. The distances of the acceptor (R6G) from the donor (C-153) in different regions of the microemulsion are different. Thus by varying the excitation wavelength (λ_{ex}) it is possible to probe the different regions of the microemulsion droplets as the location of the probe molecules in such microheterogeneous system varies depending upon their chemical properties. We showed that efficiency of FRET (short distance) is higher at a longer excitation wavelength compared to a short one. As a consequence, long distance FRET is higher at short excitation.

2. EXPERIMENTAL SECTION

2.1. Materials. Coumarin 153 (C-153) and rhodamine 6G (R6G, laser grade) were received from Exciton and used as received and CTAB was purchased from Sigma-Aldrich and was also used as received. NaAOT (sodium 1,4-bis(2-ethylhexyl) sulfosuccinate, Sigma-Aldrich) was dried under vacuum for 30 h before use. Isopropyl myristate (IPM) (SRL, India) was used as received. The RTILs *N*-methyl-*N*-propylpyrrolidinium bis(trifluoromethanesulfonyl)imide ([P_{13}][Tf_2N]) and *N*,*N*,*N*-trimethyl-*N*-propylammonium bis(trifluoromethanesulfonyl)imide ([N_{3111}][TF_2N]) were procured from Kanto Chemicals (purity> 98%) and also used as received. We have measured the water content of both the ILs using a digital automatic Karl Fischer Titrator (model VEEGO/MATIC-MD). The RTILs were clear, colorless, and odorless with a moisture content below 1 ppm for [P_{13}][Tf_2N] and 30 ppm for [N_{3111}][TF_2N]. The chemical structures of all the materials have been given in Scheme 1.

2.2. Preparation of Microemulsion. [CTA][AOT] and RTILs ([P_{13}][Tf_2N] and [N_{3111}][TF_2N]) were dried in an oven for 2 days at 70−80 °C before use. We prepared the microemulsion by taking the appropriate amount of the [CTA][AOT] in IPM. After that, we added the requisite amount of RTILs to the [CTA][AOT] in IPM. The molar ratio of RTILs/[CTA][AOT] was 0.46 and 0.92 (R) throughout all the experiments. The final concentration of [CTA][AOT] was 150 mM and the concentrations of probe molecules, C-153 and R6G, were maintained at 7 and 20 μM, respectively, in all the experiments at ambient temperature. In all the above-mentioned microemulsion [P_{13}][Tf_2N] (*N*-methyl-*N*-propylpyrrolidinium bis(trifluoromethanesulfonyl)imide) and [N_{3111}][Tf_2N] (*N*,*N*,*N*-trimethyl-*N*-propylammonium bis(trifluoromethanesulfonyl)imide) are used as RTILs, which form the pool of the microemulsion, [IPM] is used as an nonpolar solvent, and our synthesized SAIL ([CTA][AOT]) is acting as a AOT-derived surfactant.

2.3. Instrumentation. The absorption and fluorescence spectra were collected with use of a Shimadzu (model no. UV-2450) spectrophotometer and a Hitachi (model no. F-7000) spectrofluorometer, respectively. For steady-state experiments, all samples were excited at 375, 408, and 440 nm. The time-resolved emission spectra were recorded with a TCSPC picosecond spectrophotometer. The details of the time-resolved setup are described in our earlier publication.[54] In brief, the samples were excited at 408 nm by using a picosecond laser diode (IBH, Nanoled), and the signals were collected at the magic angle 54.7° with use of a Hamamatsu microchannel plate photomultiplier tube (3809U). The instrument response of our setup was 100 ps. The decay analysis was done by IBH DAS, version 6 software. All the long and short wavelength decays were fitted biexponentially by considering χ^2 becomes close to 1, indicating a good fit.

We have calculated the quantum yield of the donor molecules by following equation[55]

$$\frac{\Phi_S}{\Phi_R} = \frac{A_S}{A_R} \times \frac{(\mathrm{Abs})_R}{(\mathrm{Abs})_S} \times \frac{{n_S}^2}{{n_R}^2} \tag{1}$$

where Φ represents quantum yield, Abs represents absorbance, A represents area under the fluorescence curve, and n is the refractive index of the medium. The subscripts S and R denote the corresponding parameters for the sample and reference, respectively. The quantum yield of Rhodamine 6G in ethanol (Φ = 0.95) was taken as the reference standard.[56]

2.4. Calculation of FRET Parameters. According to the Förster theory the rate of fluorescence resonance energy transfer (k_{FRET}) can be calculated by using the following equation:[55]

$$k_{FRET} = \frac{1}{\tau^A_{rise}} = \frac{1}{\tau^0_D}\left(\frac{R_0}{R_{DA}}\right)^6 \tag{2}$$

where τ^A_{rise} is the rise time of the acceptor emission in the presence of donor and τ^0_D is the lifetime of the donor in the absence of acceptor. R_{DA} represents the distance between the molecular centers of the donor and acceptor and at a distance R_0, the efficiency of energy transfer is assumed to be 50%. R_0 is called Förster distance which is calculated from the following equation:

$$R_0 = 0.211[\kappa^2 n^{-4} Q_D J(\lambda)]^{1/6} \tag{3}$$

where n is the refractive index of the medium, Q_D is the quantum yield of the donor in the absence of acceptor, κ^2 is the orientation factor, and $J(\lambda)$ is the spectral overlap between the emission spectrum of the donor and the absorption spectrum of the acceptor. $J(\lambda)$ is related to the normalized fluorescence intensity of the donor in the absence of acceptor ($F_D(\lambda)$) and the extinction coefficient of the acceptor ($\varepsilon_A(\lambda)$) as follows:

$$J(\lambda) = \frac{\int_0^\infty F_D(\lambda)\varepsilon_A(\lambda)\lambda^4\, d\lambda}{\int_0^\infty F_D(\lambda)\, d\lambda} \tag{4}$$

In eq 3 the values of κ^2 always remain within the range 0 to 4. The zero value of κ^2 indicates the mutually perpendicular orientation of the transition dipoles which further implies the forbidden FRET process. However, in the present system as we observe the involvement of FRET, the value of κ^2 must be greater than 0. In general the value of κ^2 is taken as 2/3 for the random orientation of transition dipoles. Moreover, the calculated Förster distance is found to vary slightly in the whole range of values of κ^2. Therefore in the present system we have used κ^2 = 2/3 for the calculation of Förster distance.

3. RESULTS AND DISCUSSION

3.1. Steady-State Studies. Steady-state UV−vis absorption and fluorescence spectra of C-153 and R6G were

dx.doi.org/10.1021/jp405919y | J. Phys. Chem. B 2013, 117, 9508−9517

performed in the microemulsion systems as well as oil phase (IPM) and the results are compared to obtain an idea about the binding and location of the probe molecules. The efficient loading of the probe molecules into the microemulsion droplets can be realized from the significant red shift in the emission maximum of the probe molecule (C-153) from the nonpolar solvent IPM (λ_{emi} = 476 nm) to the microemulsion system (λ_{emi} for various microemulsions are listed in Table 1). A similar type of red shift has been reported in our earlier publication by taking C-480 as a probe molecule.[10] However, in this work for FRET study C-153 is a more suitable donor as compared to C-480 due to the higher spectral overlap between the emission spectrum of donor and the absorption spectrum of acceptor. In our characterized microemulsion, i.e., $[P_{13}][Tf_2N]$/[CTA][AOT]/[IPM] and $[N_{3111}][Tf_2N]$/[CTA][AOT]/[IPM], the emission maximum of the acceptor (R6G) does not show any dependence on excitation wavelength. This indicates that the acceptor R6G resides in a uniform environment. Because of its higher polarity, R6G is probably residing in the polar ionic pool of the RTIL microemulsion. This can be further confirmed by its single exponential decay, which is discussed in the time-resolved section. The distribution of donor, i.e., C-153, at different regions of microemulsion can be realized with variation of excitation wavelengths; the emission spectrum of the donor (C-153) exhibits a red shift with increasing excitation wavelength from 375 to 440 nm (Figure 1). The excitation at 375 nm results in the preferential excitation of the probe molecules present in the relatively nonpolar phase, while red end excitation, i.e., at ∼408 nm, resulting in the preferential excitation of the probe molecules present at the interfacial region and excitation at 440 nm, excites the molecules in the polar core of the microemulsion. Red edge excitation shift (REES) for various microemulsions with variation of R values is listed in Table 1. The 6−8 nm red shift with variation of excitation wavelength is observed for both the microemulsions, i.e., $[P_{13}][Tf_2N]$/[CTA][AOT]/[IPM] and $[N_{3111}][Tf_2N]$/[CTA][AOT]/[IPM], implying the distribution of the donor molecules. This type of red shift in microheterogeneous system is reported in the literature. Bhattacharyya and co-workers studied the

Table 1. Emission Peaks of C-153 in Different Systems with Variation of Excitation Wavelengths (REES)

system	λ_{ex}	λ_{emi}
$[P_{13}][Tf_2N]$/[CTA][AOT]/[IPM] (R = 0.46)	375	485
	408	488
	440	493
$[P_{13}][Tf_2N]$/[CTA][AOT]/[IPM] (R = 0.92)	375	489
	408	492
	440	497
$[N_{311}][Tf_2N]$/[CTA][AOT]/[IPM] (R = 0.46)	375	486
	408	488
	440	492
$[N_{311}][Tf_2N]$/[CTA][AOT]/[IPM] (R = 0.92)	375	489
	408	492
	440	497

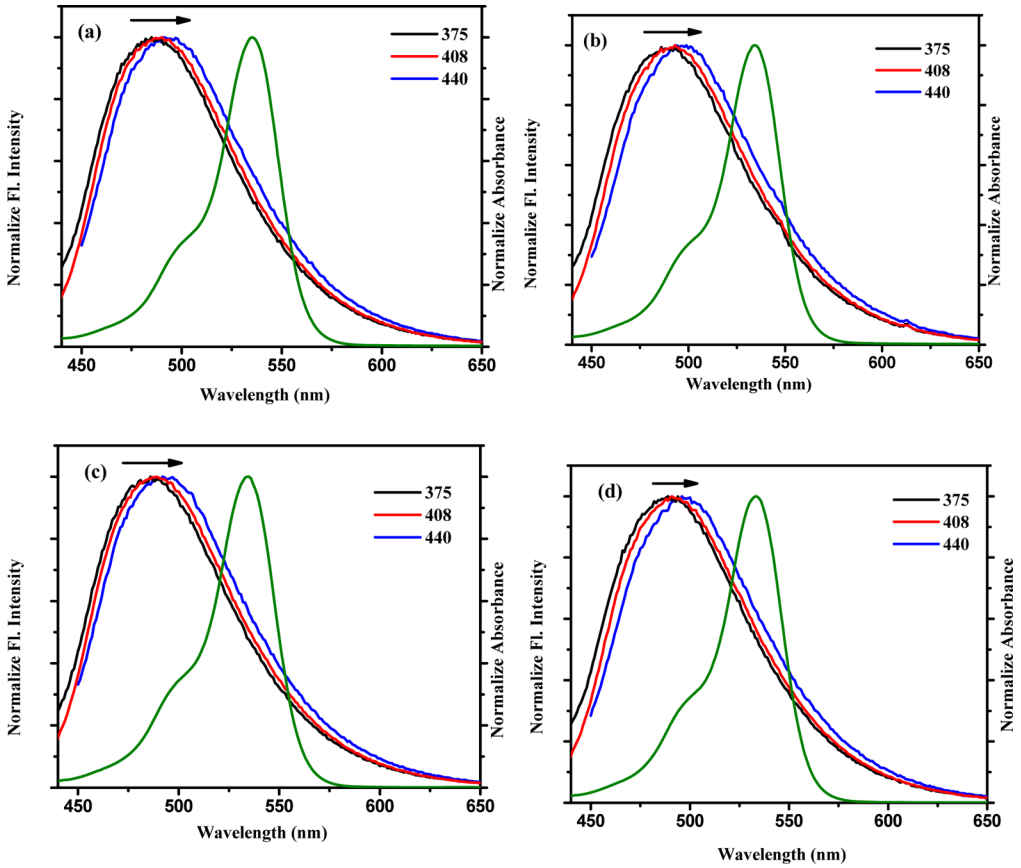

Figure 1. Absorption spectra of R6G and emission spectra of 7 μM C-153 in $[P_{13}][Tf_2N]$/[CTA][AOT]/[IPM] (a, b) and $[N_{311}][Tf_2N]$/[CTA][AOT]/[IPM] (c, d) microemulsions at R = 0.46 (a, c) and 0.92 (b, d).

dx.doi.org/10.1021/jp405919y | J. Phys. Chem. B 2013, 117, 9508−9517

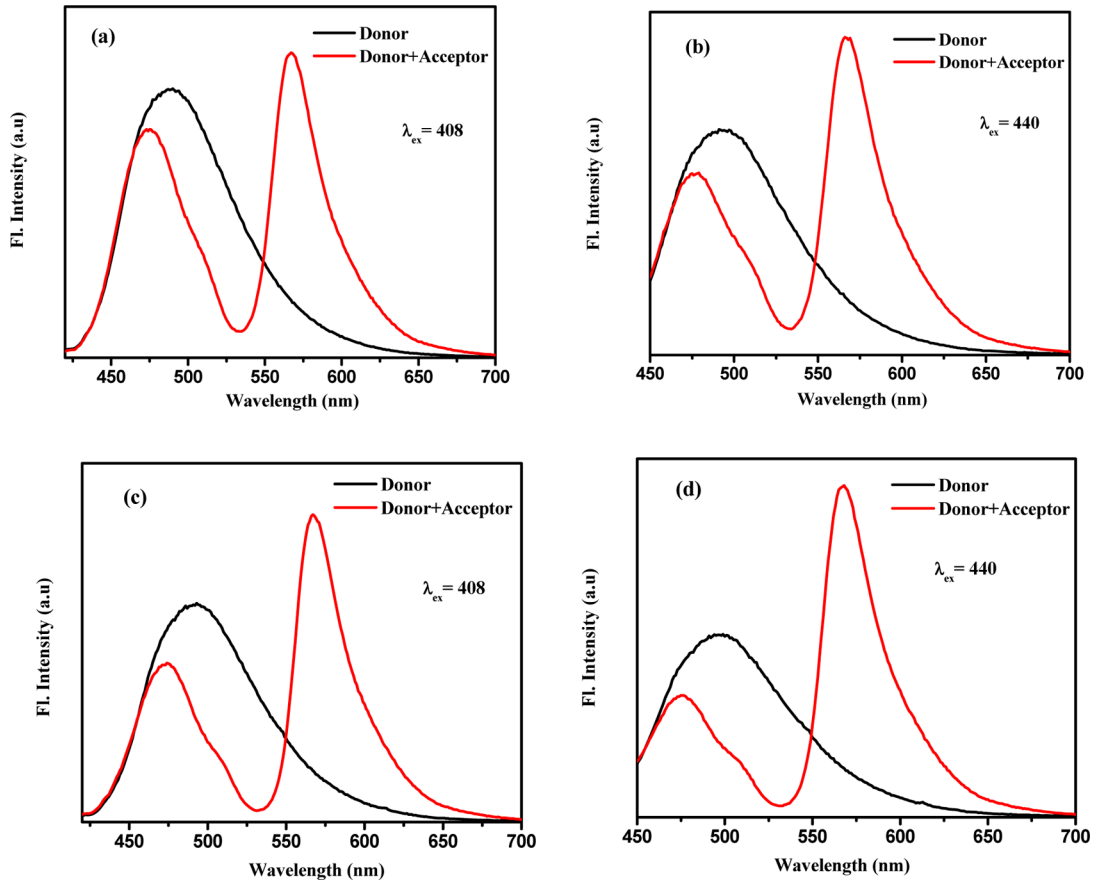

Figure 2. Emission spectra of 7 μM C-153 in the absence and presence of R6G (20 μM) in $[P_{13}][Tf_2N]$/[CTA][AOT]/[IPM] microemulsions at R = 0.46 (a, b) and 0.92 (c, d).

[pmim][BF_4]/TX-100/benzene microemulsion where the probe molecule, C480, exhibits a REES of ~6 nm upon changing the excitation wavelength from 375 to 435 nm.[34] In our earlier study on [C_2mim][C_4SO_4]/Tween-80/Span-20/IPM microemulsion with the change in excitation wavelength from 375 to 408 nm the emission maxima of C480 are found to be red-shifted ~10 nm from 450 to 460 nm.[57] The occurrence of effective FRET from the donor C-153 to the acceptor R6G at all the excitation wavelengths, i.e., at 375, 408, and 440 nm, is evident from the decrease in the steady state fluorescence intensity of the donor with addition of the acceptor and subsequent increase in the fluorescence intensity of the acceptor in the presence of the donor (Figures 2 and 3). The steady state efficiency (E) of FRET is calculated by using the following equation,[55]

$$E = 1 - \frac{F_{DA}}{F} \tag{5}$$

where F_{DA} and F denote the steady state emission intensity of the donor in the presence and absence of the acceptor, respectively. The variation of the efficiency of FRET with the change in the excitation wavelength is clearly observed from Table 2. It is evident from Table 2 that the efficiency of FRET is higher at longer wavelength in all cases. This is a consequence of the higher degree of spectral overlap between the emission spectra of donor and the absorption spectrum of the acceptor at longer excitation wavelength. The efficiency of FRET for different systems varied from 25% to 40%. Figure 1 shows the overlap between the absorption spectrum of the acceptor (R6G) with the emission spectrum of the donor (C-153) in RTILs ([P_{13}][Tf_2N] or [N_{3111}][Tf_2N])/[CTA]-[AOT]/[IPM] microemulsions at different excitation wavelengths. The values of the spectral overlap integral, $J(\lambda)$, between the emission spectrum of the donor (C-153) and absorption spectrum of the acceptor (R6G) at different excitation wavelengths are given in Table 2. Since the emission spectrum of the donor, C-153, does not change significantly with variation of the excitation wavelength from 375 to 408 nm, we have calculated and compared the $J(\lambda)$ with variation of excitation wavelengths at 408 and 440 nm. It is interesting to explain that with changes of excitation wavelength from 408 to 440 nm, $J(\lambda)$ increases for each and every microemulsions due to the REES of donor molecules. For the [P_{13}][Tf_2N]/[CTA][AOT]/[IPM] microemulsion at R = 0.46 with the variation of excitation wavelength from 408 to 440 nm the $J(\lambda)$ increases 8.4%. We have also calculated the $J(\lambda)$ for higher R value (R = 0.92) with same excitation wavelengths variation and found that it increases to 9.3%. For another RTIL-containing microemulsion, i.e., [N_{3111}][Tf_2N])/[CTA][AOT]/[IPM], the changes in the $J(\lambda)$ value with variation of the same excitation wavelengths at R = 0.46 and 0.92 are 9.1% and 8.7%. The above results ensure that with variation of excitation wavelength, $J(\lambda)$ increases irrespective of the R value. Another notable observation is that with the increase in excitation wavelength there is only an 8% to 10% increase of $J(\lambda)$. The small extent of increase of $J(\lambda)$ with an increase in the excitation wavelength can be accounted for by the dominated fluorescence intensity of the non-FRET donor.

dx.doi.org/10.1021/jp405919y | J. Phys. Chem. B 2013, 117, 9508−9517

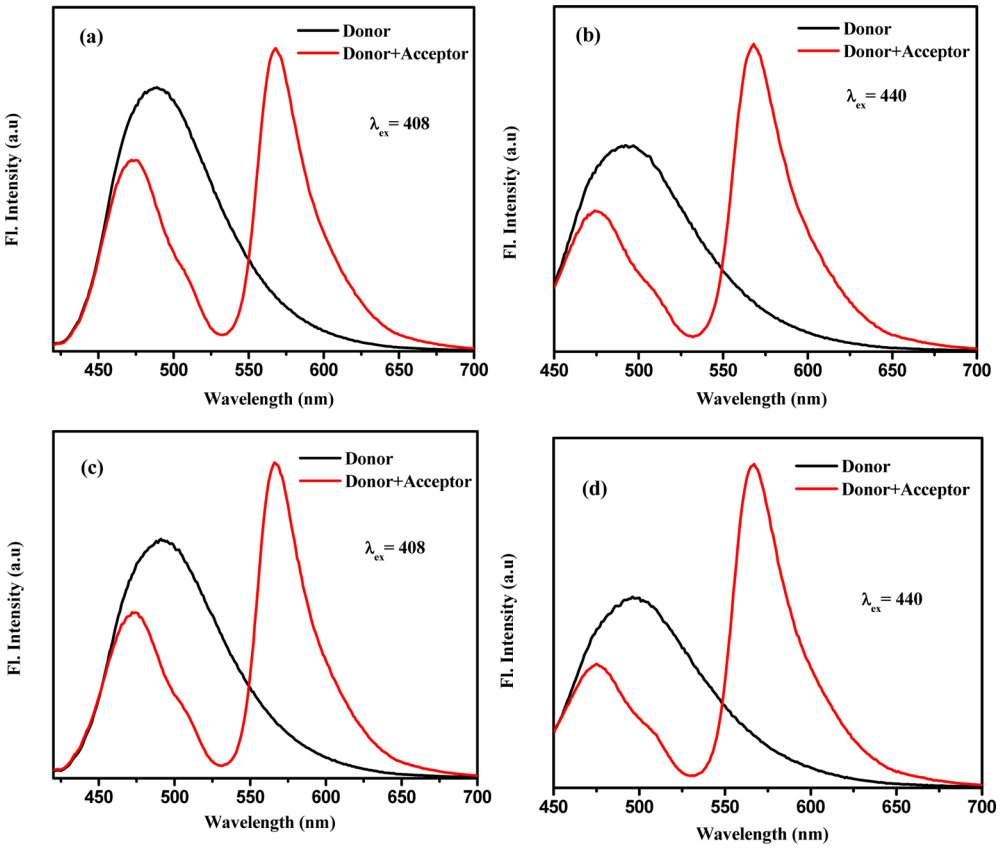

Figure 3. Emission spectra of 7 μM C-153 in the absence and presence of R6G (20 μM) in $[N_{3111}][Tf_2N]$/[CTA][AOT]/[IPM] microemulsions at R = 0.46 (a, b) and 0.92 (c, d).

Table 2. Energy Transfer Parameters for the C153-R6G Pair in Different Systems

systems	λ_{ex} (nm)	$J(\lambda)^a$ ($M^{-1}cm^{-1}$ nm^4)	R_0 (Å)	efficiency (E)^a
$[P_{13}][Tf_2N]$/[CTA] [AOT]/[IPM] (R = 0.46)	408	2.38×10^{15}	52.09	0.25
	440	2.58×10^{15}	52.79	0.28
$[P_{13}][Tf_2N]$/[CTA] [AOT]/[IPM] (R = 0.92)	408	2.48×10^{15}	51.62	0.32
	440	2.71×10^{15}	52.39	0.37
$[N_{311}][Tf_2N]$/[CTA] [AOT]/[IPM] (R = 0.46)	408	2.30×10^{15}	52.87	0.28
	440	2.51×10^{15}	53.63	0.31
$[N_{311}][Tf_2N]$/[CTA] [AOT]/[IPM] (R = 0.92)	408	2.41×10^{15}	52.68	0.33
	440	2.62×10^{15}	53.42	0.36

^{a}Experimental error of ±10%.

3.2. Time-Resolved Measurements. *3.2.1. Monitoring the Rise-Time Components of R6G.* FRET is commonly monitored by shortening of the donor's lifetime in the presence of the acceptor. However, in our case we did not observe any substantial decrease in the time-resolved decay profiles of the donor in the absence and presence of acceptor in our picoseconds experimental setup. It can be realized by considering the fact that the donor emission is dominated by unquenched non-FRET donors, hence no shortening of the donor lifetime is detected in our picoseconds setup. As the picosecond decay of the donor does not accurately describe FRET, we determined the rate of FRET from the rise time of the decay of the acceptor. However, we have to be very careful while monitoring the decay profile of acceptor, which arises only from the FRET processes because of the contribution of the donor and direct excitation of the acceptor.[58] We monitored the fluorescence transient of the acceptor (R6G) at 568 nm for both the microemulsions, i.e., $[P_{13}][Tf_2N]$/[CTA][AOT]/[IPM] and $[N_{3111}][Tf_2N]$/[CTA][AOT]/[IPM], where the contribution of the quenched emission of the donor is negligible. Figures 4 and 5 show picosecond fluorescence transients of the acceptor (R6G) in the RTILs/[CTA][AOT]/IPM microemulsions in the absence and presence of the donor (C-153) at different excitation wavelengths. In the absence of the donor (C-153), at all excitation wavelengths, the acceptor (R6G) exhibits a single exponential decay (~4210−4500 ps) with no rise component in both systems. This observation is consistent with that expected from the steady-state measurements. However, in the presence of the donor (C-153), picosecond transients of the acceptor (R6G) show distinct rise components at an excitation wavelength of 408 and 440 nm in RTIL microemulsions. As the changes of steady-state parameters on going from excitation wavelength 375 to 408 are very small we did not monitored the decays of R6G at an excitation wavelength of 375 nm. The observed rise components are ascribed to FRET from C-153 to R6G for both the excitation wavelengths (408 and 440 nm). For excitation wavelength at 408 and 440 nm, the rise components of FRET are 250 (τ_1) and 3870 ps (τ_1) in $[P_{13}][Tf_2N]$/[CTA][AOT]/[IPM] (R = 0.46) microemulsions (Figure 4 and Table 3). The time constants obtained from the exponential fitting of the decays have been given in Table 3.The greater the magnitude of the time constant of rise component,

dx.doi.org/10.1021/jp405919y | J. Phys. Chem. B 2013, 117, 9508−9517

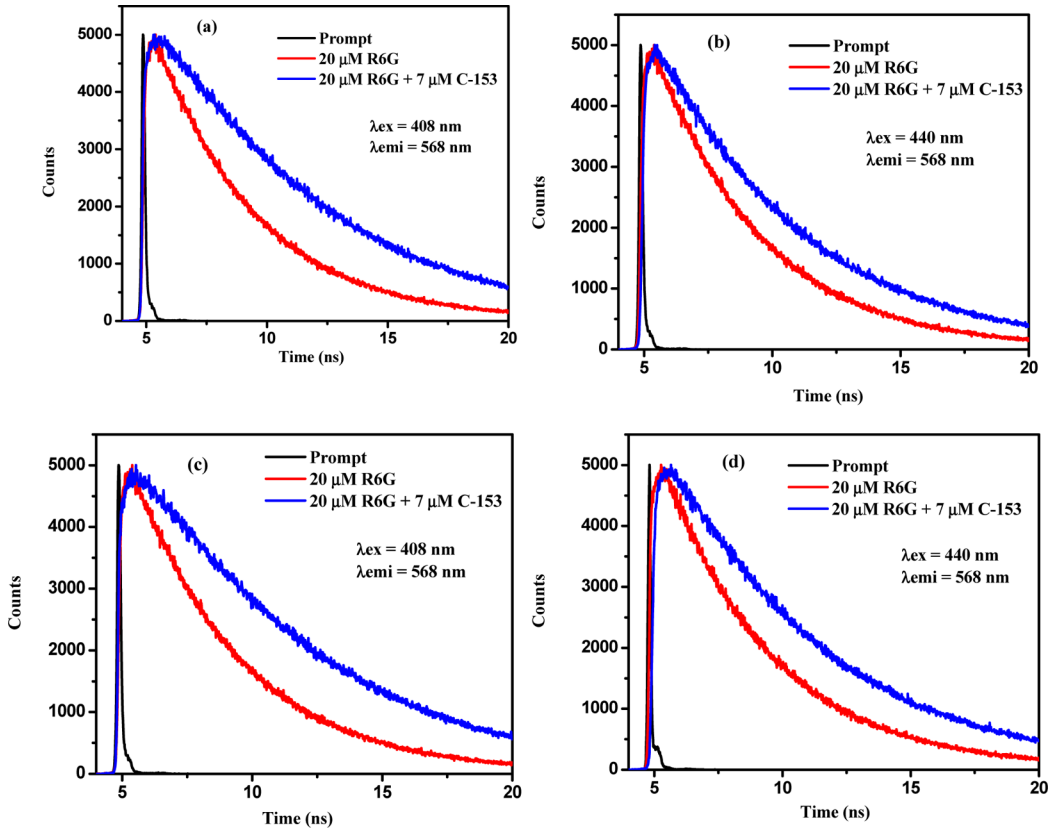

Figure 4. Time-resolved fluorescence decays of the acceptor R6G (20 μM) with (i) 0 μM C-153 and (ii) 7 μM C-153 in $[P_{13}][Tf_2N]$/[CTA][AOT]/[IPM] microemulsion at R = 0.46 (a, b) and 0.92 (c, d) with different excitation wavelengths.

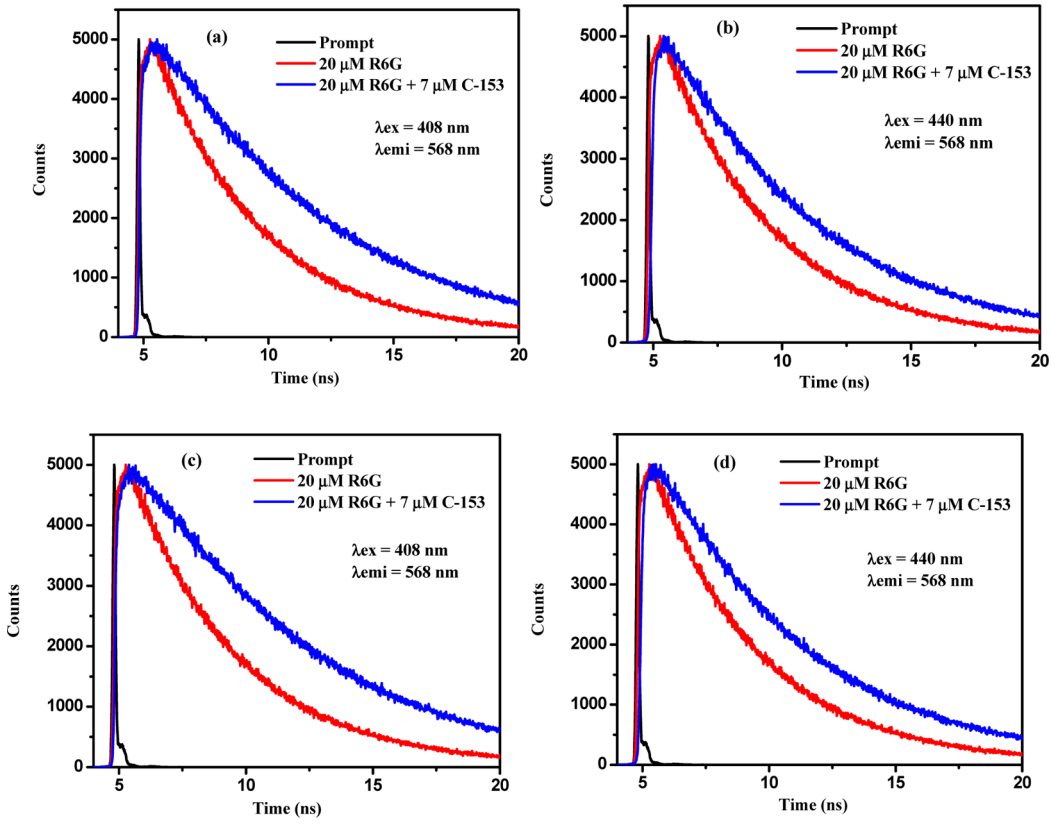

Figure 5. Time-resolved fluorescence decays of the acceptor R6G (20 μM) with (i) 0 μM C-153 and (ii) 7 μM C-153 in $[N_{3111}][Tf_2N]$/[CTA][AOT]/[IPM] microemulsion at R = 0.46 (a, b) and 0.92 (c, d) with different excitation wavelengths.

dx.doi.org/10.1021/jp405919y | J. Phys. Chem. B 2013, 117, 9508−9517

Table 3. Decay Parameters of R6G in the Presence of C-153 at Different Excitation Wavelengths

systems	λ_{ex} (nm)	$\tau_1(a_1)^a$	$\tau_2(a_2)^a$	$\tau_3(a_3)^a$
$[P_{13}][Tf_2N]$/[CTA] [AOT]/[IPM] (R = 0.46)	408	0.25 (−0.14, 11.6%)	3.87 (−1.07, 88.4%)	5.57 (2.22)
	440	0.25 (−0.12, 57.2%)	3.87 (−0.09, 42.8%)	5.57 (1.22)
$[P_{13}][Tf_2N]$/[CTA] [AOT]/[IPM] (R = 0.92)	408	0.25 (−0.09, 11.5%)	3.37 (−0.69, 88.5%)	5.77 (1.78)
	440	0.25 (−0.20, 50.0%)	3.37 (−0.20, 50.0%)	5.77 (1.40)
$[N_{311}][Tf_2N]$/[CTA] [AOT]/[IPM] (R = 0.46)	408	0.30 (−0.13, 11.5%)	3.93 (−1.00, 88.5%)	5.57 (2.13)
	440	0.30 (−0.09, 50%)	3.93 (−0.09, 50%)	5.57 (1.32)
$[N_{311}][Tf_2N]$/[CTA] [AOT]/[IPM] (R = 0.92)	408	0.34 (−0.08, 10.6%)	3.45 (−0.67, 89.4%)	5.79 (1.75)
	440	0.34 (−0.15, 78.9%)	3.45 (−0.04, 21.1%)	5.79 (1.19)

[a]Experimental error of ±5%.

the longer is the distance between donor and acceptor. Now, for the same microemulsion at R = 0.92 the rise component changes to 250 (τ_1) and 3370 ps (τ_2). The decrease in lifetime (τ_2) on going from lower to higher R value is a manifestation of the movement of the donor molecules toward the pool of the microemulsion. To confirm this observation we also performed the same experiment with another RTIL-containing microemulsion, i.e., $[N_{3111}][Tf_2N]$/[CTA][AOT]/[IPM], and found that the rise components were 300 (τ_1) and 3930 ps (τ_2) at R = 0.46, which changed to 340 (τ_1) and 3450 ps (τ_2) at R = 0.92 (Figure 5, Table 3). Hence, we can generalize our statement that on going from lower to higher R value the lifetime (τ_2) decreases for both the microemulsions studied here. As the ionic liquid content increases with increase in R values the probe molecules are shifted toward the polar core of the microemulsion, which results in an increase in contribution of the faster time scale of FRET and a decrease in contribution of the slower time scale of FRET.

3.2.2. Excitation Wavelength Dependence Study. Another interesting aspect in this article is excitation wavelength dependence of FRET to monitor the structural heterogeneity of the $[P_{13}][Tf_2N]$/[CTA][AOT]/[IPM] and $[N_{3111}][Tf_2N]$/[CTA][AOT]/[IPM] microemulsion systems. Picosecond decay parameters of R6G in the presence of C-153 at different excitation wavelengths are shown in Table 3. For $[P_{13}][Tf_2N]$/[CTA][AOT]/[IPM] (R = 0.46) microemulsion, an excitation wavelength of 408 nm shows two FRET components 250 (11.6%) and 3870 ps (88.4%) (Table 3). Now, at an excitation wavelength of 440 nm the components remained unchanged although the contribution of each component changes drastically. The contribution of the faster component changes from 11.6% to 57.2% and that of the slower FRET component changes from 88.4% to 42.8%. We have also performed similar experiments with higher R value. For the same microemulsion at R = 0.92 the FRET components are 250 (11.5%) and 3370 ps (88.5%) at an excitation wavelength of 408 nm. The contribution of both components again changes with keeping the same time constant of FRET. The contribution of the faster FRET component changes from 11.5% to 50.0% and that of the slower FRET component changes from 88.5% to 50.0%. From the above two results it is obvious that the effect of excitation wavelength on FRET is the same with variation of R. The increase in contribution of the fast component or the decrease in contribution of the slow component of FRET can be understood by considering the fact that with an increase in excitation wavelength there is a marked increase in the contribution of the donor in the interfacial region where FRET occurs very fast (because of the short D−A distance). Now, to further support the above facts we applied the same experiments with another microemulsion, i.e., $[N_{3111}][Tf_2N]$/[CTA][AOT]/[IPM], where RTIL has been changed from $[P_{13}][Tf_2N]$ to $[N_{3111}][Tf_2N]$. Here we also performed the excitation wavelength dependence with variation of R values. At R = 0.46 with an excitation of 408 nm the FRET components are found to be 300 (11.5%) and 3930 ps (88.5%). Now, at an excitation of 440 nm the contribution of the FRET components changes from 11.5% to 50.0% and 88.5% to 50.0%. However, at higher R value i.e., R = 0.92, the change of faster and slower FRET components is relatively higher, where it changes from 10.6% and 89.4% with an excitation of 408 nm to 78.9% to 21.1% with an excitation 440 nm. Hence it is clear that the effect of excitation wavelength for both the microemulsions, i.e., $[P_{13}][Tf_2N]$/[CTA][AOT]/[IPM] and $[N_{3111}][Tf_2N]$/[CTA][AOT]/[IPM], is similar.

3.2.3. Multiple Distances Dependent FRET. In the present work we have also shown multiple time scales of FRET resulting from the different distribution of the donors with respect to the acceptor which is present in the ionic liquid pool of the microemulsions (we did not obtain any spectral shift of acceptor with variation of excitation wavelength implying the homogeneous distribution of R6G). From the time constant of FRET, the donor−acceptor distances, R_{DA}, were calculated with the help of eq 2. The calculated values are listed in Table 4.

Table 4. Donor−Acceptor Distances of C-153 and R6G Pairs in the Various Microemulsions

systems	λ_{ex} (nm)	τ_{FRET}	R_{DA} (Å)[a]
$[P_{13}][Tf_2N]$/[CTA][AOT]/[IPM] (R = 0.46)	408	0.25, 3.87	31.9, 43.0
	440	0.25, 3.87	32.4, 43.6
$[P_{13}][Tf_2N]$/[CTA][AOT]/[IPM] (R = 0.92)	408	0.25, 3.37	31.6, 49.2
	440	0.25, 3.37	32.1, 49.9
$[N_{311}][Tf_2N]$/[CTA][AOT]/[IPM] (R = 0.46)	408	0.30, 3.93	33.5, 51.3
	440	0.30, 3.93	33.9, 52.0
$[N_{311}][Tf_2N]$/[CTA][AOT]/[IPM] (R = 0.92)	408	0.34, 3.45	34.0, 50.2
	440	0.34, 3.45	34.5, 50.9

[a]Experimental error of ±10%.

This corresponds to two distinct D−A distances of ∼31−35 and ∼43−51 Å. These distances are smaller than the size of the microemulsion that we reported earlier.[10] The ∼43−51 Å distance arises from a donor residing in the outer periphery of the microemulsion to an acceptor inside the polar RTIL pool and $R_{DA} \approx$ 31−35 Å corresponds to a situation where the acceptor is in the RTIL pool and the donor is residing in between the surfactant chain of the microemulsion and the RTIL pool (interfacial region). In our picosecond setup we are unable to detect the ultrafast FRET components due to limited

dx.doi.org/10.1021/jp405919y | J. Phys. Chem. B 2013, 117, 9508−9517

instrumental resolution where R_{DA} corresponds to the sum of radii of the donor and the acceptor molecules.

4. CONCLUSION

We have studied FRET between coumarin-153 (donor) and rhodamine 6G (acceptor) by observing the rise time of the acceptor (R6G) emission in our earlier characterized novel IL/O microemulsions where the polar core of the ionic liquid, $[P_{13}][Tf_2N]$ and $[N_{3111}][Tf_2N]$, is stabilized by a SAIL ([CTA][AOT]) in a biological oil phase of IPM. It is showed that with an increase in excitation wavelength, the contribution of FRET from the donor in the polar region (picosecond component) increases and that due to donor in the nonpolar region (nanosecond component) decreases. We have also performed similar experiments with variation of R, and eventually we have shown that the effect of excitation wavelength is similar irrespective of R. We believe our present study helps to understand various processes occurring in biological molecules embedded in biomembranes as these aggregates have the potential to serve as good biomimicry models as well as drug delivery systems. Recently we have shown that the microemulsion composed of SAIL, as a surfactant, RTIL, as a polar core solvent and IPM as a nonpolar solvent, exhibits stability over a wide range of temperatures (278 to ≥423 K).[53] Hence, further studies of FRET at very high and low temperatures is currently being pursued in our laboratory.

AUTHOR INFORMATION

Corresponding Author

*E-mail: nilmoni@chem.iitkgp.ernet.in. Fax: 91-3222-255303.

Notes

The authors declare no competing financial interest.

ACKNOWLEDGMENTS

N.S. is thankful to Council of Scientific and Industrial Research (CSIR) for a generous research grant. C.B. and J.K.are thankful to UGC and S.M. and S.G. are thankful to CSIR for their research fellowships.

REFERENCES

(1) *Ionic Liquids: Industrial Applications for Green Chemistry*; Rogers, R. D., Seddon, K. R, Eds.; ACS Symposium Series 818; American Chemical Society: Washington, DC, 2002.

(2) *Ionic Liquids III: Fundamentals, Challenges, and Opportunities*; Rogers, R. D., Seddon, K. R, Eds.; ACS Symposium Series 901; American Chemical Society: Washington, DC, 2005.

(3) Baker, G. A.; Baker, S. N.; Pandey, S.; Bright, F. V. An Analytical View of Ionic Liquids. *Analyst* **2005**, *130*, 800−808.

(4) Hallett, J. P.; Welton, T. Room-Temperature Ionic Liquids: Solvents for Synthesis and Catalysis. 2. *Chem. Rev.* **2011**, *111*, 3508−3576.

(5) Seddon, K. R. Ionic Liquids: a Taste of the Future. *Nat. Mater.* **2003**, *2*, 363−364.

(6) Rantwijk, F.; van Sheldon, R. A. Biocatalysis in Ionic Liquids. *Chem. Rev.* **2007**, *107*, 2757−2785.

(7) Rogers, R. D.; Seddon, K. R. Ionic liquids—Solvents of the Future? *Science* **2003**, *302*, 792−793.

(8) Brown, P.; Butts, C. P.; Eastoe, J.; Grillo, I.; James, C.; Khan, A. New Catanionic Surfactants with Ionic Liquid Properties. *J. Colloid Interface Sci.* **2013**, *395*, 185−189.

(9) Rao, V. G.; Ghosh, S.; Ghatak, C.; Mandal, S.; Brahmachari, U.; Sarkar, N. Designing a New Strategy for the Formation of IL-in-Oil Microemulsions. *J. Phys. Chem. B* **2012**, *116*, 2850−2855.

(10) Banerjee, C.; Mandal, S.; Ghosh, S.; Kuchlyan, J.; Kundu, N.; Sarkar, N. Unique Characteristics of Ionic Liquids Comprised of Long-Chain Cations and Anions: A New Physical Insight. *J. Phys. Chem. B* **2013**, *117*, 3927−3934.

(11) Dubertret, M.; Calame, M.; Libchaber, A. J. Single-Mismatch Detection using Gold-Quenched Fluorescent Oligonucleotides. *Nat. Biotechnol.* **2001**, *19*, 365−370.

(12) Patolsky, F.; Gill, R.; Weizmann, Y.; Mokari, T.; Banin, U.; Willner, I. Lighting-up the Dynamics of Telomerization and DNA Replication by CdSe-ZnS Quantum Dots. *J. Am. Chem. Soc.* **2003**, *125*, 13918−13919.

(13) Oh, E.; Hong, M.-Y.; Lee, D.; Nam, S.-H.; Yoon, H. C.; Kim, H.-S. Inhibition Assay of Biomolecules Based on Fluorescence Resonance Energy Transfer (FRET) between Quantum Dots and Gold Nanoparticles. *J. Am. Chem. Soc.* **2005**, *127*, 3270−3271.

(14) Deniz, A. A.; Dahan, M.; Grunwell, J. R.; Ha, T.; Faulhaber, A. E.; Chemla, D. S.; Weiss, S.; Schultz, P. G. Single-Pair Fluorescence Resonance Energy Transfer on Freely Diffusing Molecules: Observation of Förster Distance Dependence and Subpopulations. *Proc. Natl. Acad. Sci.* **1999**, *96*, 3670−3675.

(15) Ha, T.; Ting, A. Y.; Liang, J.; Caldwell, W. B.; Deniz, A. A.; Chemla, D. S.; Schultz, P. G.; Weiss, S. Single-Molecule Fluorescence Spectroscopy of Enzyme Conformational Dynamics and Cleavage Mechanism. *Proc. Natl. Acad. Sci.* **1999**, *96*, 893−898.

(16) Haugland, R. P.; Yguerabide, J.; Stryer, L. Dependence of the Kinetics of Singlet-Singlet Energy Transfer on Spectral Overlap. *Proc. Natl. Acad. Sci.* **1969**, *63*, 23−30.

(17) Clapp, A. R.; Medintz, I. L.; Mauro, J. M.; Fisher, B. R.; Bawendi, M. G.; Mattoussi, H. Fluorescence Resonance Energy Transfer Between Quantum Dot Donors and Dye-Labeled Protein Acceptors. *J. Am. Chem. Soc.* **2004**, *126*, 301−310.

(18) Saini, S.; Bhowmick, S.; Shenoy, B. V.; Bagchi, B. Rate of Excitation Energy Transfer between Fluorescent Dyes and Nanoparticles. *J. Photochem. Photobiol., A* **2007**, *190*, 335−341.

(19) Scholes, G. D.; Jordanides, X. J.; Fleming, G. R. Adapting the Förster Theory of Energy Transfer for Modeling Dynamics in Aggregated Molecular Assemblies. *J. Phys. Chem. B* **2001**, *105*, 1640−1651.

(20) Wong, K. F.; Bagchi, B.; Rossky, P. J. Distance and Orientation Dependence of Excitation Transfer Rates in Conjugated Systems: Beyond the Förster Theory. *J. Phys. Chem. A* **2004**, *108*, 5752−5763.

(21) Jordanides, X. J.; Scholes, G. D.; Fleming, G. R. The Mechanism of Energy Transfer in the Bacterial Photosynthetic Reaction Center. *J. Phys. Chem. B* **2001**, *105*, 1652−1669.

(22) Scholes, G. D.; Fleming, G. R. On the Mechanism of Light Harvesting in Photosynthetic Purple Bacteria: B800 to B850 Energy Transfer. *J. Phys. Chem. B* **2000**, *104*, 1854−1868.

(23) Krueger, B. P.; Scholes, G. D.; Fleming, G. R. Calculation of Couplings and Energy-Transfer Pathways between the Pigments of LH2 by the ab Initio Transition Density Cube Method. *J. Phys. Chem. B* **1998**, *102*, 5378−5386.

(24) Dayal, S.; Lou, Y. B.; Samia, A. C. S.; Berlin, J.; Kenney, M. E.; Burda, C. Observation of Non-Förster-Type Energy-Transfer Behavior in Quantum Dot-Phthalocyanine Conjugates. *J. Am. Chem. Soc.* **2006**, *128*, 13974−13975.

(25) Mandal, S.; Ghatak, C.; Rao, V. G.; Ghosh, S.; Sarkar, N. Pluronic Micellar Aggregates Loaded with Gold Nanoparticles (Au NPs) and Fluorescent Dyes: A Study of Controlled Nanometal Surface Energy Transfer. *J. Phys. Chem. C* **2012**, *116*, 5585−5597.

(26) Saini, S.; Srinivas, G.; Bagchi, B. Distance and Orientation Dependence of Excitation Energy Transfer: From Molecular Systems to Metal Nanoparticles. *J. Phys. Chem. B* **2009**, *113*, 1817−1832.

(27) Saini, S.; Shenoy, V. B.; Bagchi, B. Excitation Energy Transfer between Non-Spherical Metal Nanoparticles: Effects of Shape and Orientation on Distance Dependence of Transfer Rate. *J. Phys. Chem. C* **2008**, *112*, 6299−6306.

(28) Krueger, B. P.; Scholes, G. D.; Fleming, G. R. Calculation of Couplings and Energy-Transfer Pathways between the Pigments of

LH2 by the ab Initio Transition Density Cube Method. *J. Phys. Chem. B* **1998**, *102*, 5378−5385.
(29) Sen, T.; Jana, S.; Koner, S.; Patra, A. Energy Transfer between Confined Dye and Surface Attached Au Nanoparticles of Mesoporous Silica. *J. Phys. Chem. C* **2010**, *114*, 707−714.
(30) Das, A. K.; Mondal, T.; Sasmal, D. K.; Bhattacharyya, K. Femtosecond Study of Ultrafast Fluorescence Resonance Energy Transfer in a Catanionic Vesicle. *J. Chem. Phys.* **2011**, *135*, 074507−074513.
(31) Sahu, K.; Ghosh, S.; Mondal, S. K.; Ghosh, B. C.; Sen, P.; Roy, D.; Bhattacharyya, K. Ultrafast Fluorescence Resonance Energy Transfer in a Micelle. *J. Chem. Phys.* **2006**, *125*, 044714−044721.
(32) Ghosh, S.; Dey, S.; Adhikari, A.; Mandal, U.; Bhattacharyya, K. Ultrafast Fluorescence Resonance Energy Transfer in the Micelle and the Gel Phase of a PEO-PPO-PEO Triblock Copolymer: Excitation Wavelength Dependence. *J. Phys. Chem. B* **2007**, *111*, 7085−7091.
(33) Das, D. K.; Das, A. K.; Mondal, T.; Mandal, A. K.; Bhattacharyya, K. Ultrafast FRET in Ionic Liquid-P123 Mixed Micelles: Region and Counterion Dependence. *J. Phys. Chem. B* **2010**, *114*, 13159−13166.
(34) Adhikari, A.; Das, D. K.; Sasmal, D. K.; Bhattacharyya, K. Ultrafast FRET in a Room Temperature Ionic Liquid Microemulsion: A Femtosecond Excitation Wavelength Dependence Study. *J. Phys. Chem. A* **2009**, *113*, 3737−3743.
(35) Kahlweit, M.; Strey, R. Phase Behavior of Ternary Systems of the Type H_2O Oil Nonionic Amphiphile (Microemulsions). *Angew. Chem., Int. Ed.* **1985**, *24*, 654−668.
(36) Kahlweit, M.; Strey, R.; Firman, P.; Haase, D.; Jen, J.; Schomacker, R. General Patterns of the Phase Behavior of Mixtures of Water, Nonpolar Solvents, Amphiphiles, and Electrolytes. 1. *Langmuir* **1988**, *4*, 499−511.
(37) Kahlweit, M.; Strey, R.; Firman, P. Search for Tricritical Points in Ternary Systems: Water-Oil-Nonionic Amphiphile. *J. Phys. Chem.* **1986**, *90*, 671−677.
(38) Kahlweit, M.; Strey, R.; Busse, G. Microemulsions: A Qualitative Thermodynamic Approach. *J. Phys. Chem.* **1990**, *94*, 3881−3894.
(39) Gao, H. X.; Li, J. C.; Han, B. X.; Chen, W. N.; Zhang, J. L.; Zhang, R. Microemulsions with Ionic Liquid Polar Domains. *Phys. Chem. Chem. Phys.* **2004**, *6*, 2914−2916.
(40) Fletcher, K. A.; Pandey, S. Surfactant Aggregation within Room-Temperature Ionic Liquid 1-Ethyl-3-methylimidazolium bis-(trifluoromethylsulfonyl)imide. *Langmuir* **2004**, *20*, 33−36.
(41) Cheng, S.; Zhnag, J.; Zhang, Z.; Han, B. Novel Microemulsions: Ionic Liquid-in-Ionic Liquid. *Chem. Commun.* **2007**, 2497−2499.
(42) Gao, Y.; Han, S.; Han, B.; Li, G.; Shen, D.; Li, Z.; Du, J.; Hou, W.; Zhang, G. TX-100/Water/1-Butyl-3-methylimidazolium Hexafluorophosphate Microemulsions. *Langmuir* **2005**, *21*, 5681−5684.
(43) Eastoe, J.; Gold, S.; Rogers, S. E.; Paul, A.; Welton, T.; Heenan, R. K.; Grillo, I. Ionic Liquid-in-Oil Microemulsions. *J. Am. Chem. Soc.* **2005**, *127*, 7302−7303.
(44) Li, N.; Zhang, S.; Zheng, L.; Gao, Y.; Yu, L. Second Virial Coefficient of bmimBF4/Triton X-100/Cyclohexane Ionic Liquid Microemulsion as Investigated by Microcalorimetry. *Langmuir* **2008**, *24*, 2973−2976.
(45) Behera, K.; Pandey, S. Concentration-Dependent Dual Behavior of Hydrophilic Ionic Liquid in Changing Properties of Aqueous Sodium Dodecyl Sulfate. *J. Phys. Chem. B* **2007**, *111*, 13307−13315.
(46) Behera, K.; Pandey, D. M.; Porel, M.; Pandey, S. Unique Role of Hydrophilic Ionic Liquid in Modifying Properties of Aqueous Triton X-100. *J. Chem. Phys.* **2007**, *127*, 184501−184510.
(47) Rai, R.; Baker, A. G.; Behera, K.; Mohanty, P.; Kurur, D. N.; Pandey, S. Ionic Liquid-Induced Unprecedented Size Enhancement of Aggregates within Aqueous Sodium Dodecylbenzene Sulfonate. *Langmuir* **2010**, *26*, 17821−17826.
(48) Rai, R.; Pandey, S.; Baker, N. S.; Vora, S.; Behera, K.; Baker, A. G.; Pandey, S. Ethanol-Assisted, Few Nanometer, Water-In-Ionic-Liquid Reverse Micelle Formation by a Zwitterionic Surfactant. *Chem.—Eur. J.* **2012**, *18*, 12213−12217.
(49) Eastoe, J.; Gold, S.; Rogers, S.; Wyatt, P.; Steytler, D. C.; Gurgel, A.; Heenan, R. K.; Fan, X.; Beckman, E. J.; Enick, R. M. Designed CO_2-Philes Stabilize Water-in-Carbon Dioxide Microemulsions. *Angew. Chem., Int. Ed.* **2006**, *45*, 3675−3677.
(50) Moniruzzamana, M.; Tamuraa, M.; Taharaa, Y.; Kamiya, N.; Goto, M. Ionic Liquid-in-Oil Microemulsion as a Potential Carrier of Sparingly Soluble Drug: Characterization and Cytotoxicity Evaluation. *Int. J. Pharm.* **2010**, *400*, 243−250.
(51) Yang, F.; Kamiya, N.; Goto, M. Transdermal Delivery of the Anti-Rheumatic Agent Methotrexate Using a Solid-in-Oil Nanocarrier. *Eur. J. Pharm. Biopharm.* **2012**, *82*, 158−163.
(52) Saha, R.; Rakshit, S.; Mitra, R. K.; Pal, S. K. Microstructure, Morphology, and Ultrafast Dynamics of a Novel Edible Micro-emulsion. *Langmuir* **2012**, *28*, 8309−8317.
(53) Rao, V. G.; Banerjee, C.; Ghosh, S.; Mandal, S.; Kuchlyan, J.; Sarkar, N. A Step toward the Development of High-Temperature Stable Ionic Liquid-in-Oil Microemulsions Containing Double-Chain Anionic Surface Active Ionic Liquid. *J. Phys. Chem. B* **2013**, *117*, 7472−7480.
(54) Hazra, P.; Chakrabarty, D.; Sarkar, N. Solvation Dynamics of Coumarin 153 in Aqueous and Non-aqueous Reverse Micelles. *Chem. Phys. Lett.* **2003**, *371*, 553−562.
(55) Lakowicz, J. R. *Principles of Fluorescence Spectroscopy*; Plenum: New York, NY, 1999; Vol. 2.
(56) Magde, D.; Wong, R.; Seybold, P. G. Fluorescence Quantum Yields and Their Relation to Lifetimes of Rhodamine 6G and Fluorescein in Nine Solvents: Improved Absolute Standards for Quantum Yields. *Photochem. Photobiol.* **2002**, *75*, 327−334.
(57) Mandal, S.; Ghosh, S.; Banerjee, C.; Kuchlyan, J.; Banik, D.; Sarkar, N. A Novel Ionic Liquid-in-Oil Microemulsion Composed of Biologically Acceptable Components: An Excitation Wavelength Dependent Fluorescence Resonance Energy Transfer Study. *J. Phys. Chem. B* **2013**, *117*, 3221−3231.
(58) Rao, V. G.; Mandal, S.; Ghosh, S.; Banerjee, C.; Sarkar, N. Study of Fluorescence Resonance Energy Transfer in Zwitterionic Micelle: Ionic-Liquid-Induced Changes in FRET Parameters. *J. Phys. Chem. B* **2012**, *116*, 12021−12029.